Liquid Crystals

Responsive Photonic Liquid Marbles

Manos Anyfantakis,* Venkata S. R. Jampani, Rijeesh Kizhakidathazhath, Bernard P. Binks, and Jan P. F. Lagerwall*

Abstract: *Liquid marbles have potential to serve as mini-reactors for fabricating new materials, but this has been exploited little and mostly for conventional chemical reactions. Here, we uncover the unparalleled capability of liquid marbles to act as platforms for controlling the self-assembly of a bio-derived polymer, hydroxypropyl cellulose, into a cholesteric liquid crystalline phase showing structural coloration by Bragg reflection. By adjusting the cholesteric pitch via quantitative water extraction, we achieve liquid marbles that we can tailor for structural color anywhere in the visible range. Liquid marbles respond with color change that can be detected by eye, to changes in temperature, exposure to toxic chemicals and mechanical deformation. Our concept demonstrates the advantages of using liquid marbles as a miniature platform for controlling the liquid crystal self-assembly of bio-derived polymers, and their exploitation to fabricate sustainable, responsive soft photonic objects.*

Introduction

Liquid marbles (LMs) are sessile drops of liquids coated by solvophobic particles.[1] They bear resemblance to Pickering emulsions[2] (water + oil), albeit with a gaseous rather than liquid continuous phase, and they may be viewed as the macroscopic analogue of dry water,[3] a phase inverted aqueous foam. When a particle of radius r (initially dispersed in either air or water) is adsorbed at an air–water interface, a portion of the fluid interface is lost, and a new particle-water interface is created. If the particle contact angle at the liquid-air interface is θ (measured into water) and the surface tension is γ_{LG}, the change in surface free energy upon particle adsorption to the interface is $\Delta E = -\pi r^2 \gamma_{LG}(1 \pm \cos\theta)^2$; the

sign in the parenthesis is negative (resp. positive) for particle adsorption from the water (resp. air) phase.[4] Therefore, the free energy of the system is always reduced (or unchanged for $\theta = 0°$ or 180°) upon particle adsorption and this process is thermodynamically favorable.

The particle coating gives LMs most of their remarkable properties.[5, 6] For instance, LMs behave as non-wetting soft solids because the encapsulated liquid does not contact any supporting substrate, regardless of whether it is solid or liquid.[1] This extraordinary feature led to the extensive exploitation of LMs to transport liquids across substrates without leakage and requiring forces that are much smaller than what is needed for transporting a wetting liquid.[1] Numerous manipulation strategies have been proposed,[7,8] including actuation driven by external stimuli[9] such as magnetic fields[10,11] and light.[12,13] Another notable property of LMs is that they can communicate with their environment. First, the coating particles can interact with both surrounding phases, as both are in direct contact. More interestingly, the isolated core liquid and the fluid surrounding phase (air or another liquid) can also interact, because most LMs are coated by disordered particle layers that incorporate voids.[7,14] These properties provided the basis for many sensing applications, from color change-based qualitative detection of different gases by LMs containing indicators[15] to the quantitative identification of target analytes via the coupling of plasmonic LMs and surface-enhanced Raman spectroscopy.[16]

The thought-provoking idea of using LMs as micro-reactors for creating new materials was foreseen soon after their discovery.[7] Exploiting LMs for chemical synthesis has numerous advantages (reduced amounts of reagents and reaction times), which are a consequence of their small volume.[6] This concept was first materialized by Xue et al. who used magnetic LMs that could be opened and closed on demand, allowing for reaction and analysis to be done in a single platform.[17] Several examples of chemical reactions have followed,[18] clearly proving the validity of this promising concept.

A natural extension of the micro-reactor concept is to go beyond chemical synthesis and exploit LMs as a miniature platform for guiding the self-assembly of building blocks into materials with programmable functions. Despite its ground-breaking potential, this concept has been used very rarely. A unique demonstration was reported by Gu et al. who prepared LMs in which the core liquid was a mixture of a colloidal suspension of monodisperse nanoparticles (NPs) and a photosensitive polymer precursor. UV curing of the LM interior followed by ultrasonication to remove the coating microparticles led to non-iridescent colored LMs.[19] This is an

[*] Dr. M. Anyfantakis, Dr. V. S. R. Jampani, Dr. R. Kizhakidathazhath,
Prof. J. P. F. Lagerwall
Department of Physics and Materials Science
University of Luxembourg
162a Avenue de la Faïencerie, 1511 Luxembourg (Luxembourg)
E-mail: anyfas.com@gmail.com
           jan.lagerwall@lcsoftmatter.com

Prof. B. P. Binks
Department of Chemistry and Biochemistry
University of Hull, HU6 7RX, Hull (UK)

Supporting information and the ORCID identification number(s) for the author(s) of this article can be found under:
https://doi.org/10.1002/anie.202008210.

example of structural color, which results from the physical interaction of visible light with a material encompassing a periodicity in refractive index of the order of the light wavelength.[20] In this case,[19] this was due to the self-assembly of the silica NPs into a colloidal photonic crystal.[21]

An alternative self-assembly route to produce materials that display structural color is to use anisometric building blocks that can form cholesteric liquid crystal (LC) phases. Typically, chiral rod-like building blocks adopt a parallel orientation to a common axis (called the director), locally developing a nematic order. However, due to chiral inter-actions between the building blocks, the director undergoes a helicoidal modulation along a single axis that is itself perpendicular to the director. The cholesteric pitch P (the distance along the helix over which the director performs a 360° turn) and its handedness characterize this helicoidal arrangement. In cholesteric materials where P assumes sub-micrometer values, illumination with white light results in the visible selective reflection of a narrow wavelength band, leading to structural color. According to Bragg's law, the central reflection wavelength (as measured in air) is $\lambda = n_{av}P\cos\alpha$, where n_{av} is the average refractive index of the phase and α is the angle between the illumination/viewing direction and the helix axis.[22,23]

Cellulose, the most abundant biopolymer, and its various relatives (polysaccharides of similar structure like chitin) and derivatives (polymers directly derived from cellulose) are excellent candidates as cholesteric building blocks,[24] as evidenced from their extensive use by nature to form structures with unique photonic properties.[25] Cellulose-based materials are generally biocompatible, biodegradable, highly abundant and cost-effective. An interesting example is hydroxypropyl cellulose (HPC), a water-soluble cellulose ether in which some of the hydroxyl groups have been propylated ($-OCH_2CH(OH)CH_3$).[26] Concentrated aqueous HPC solutions form a cholesteric LC phase,[27] which results from the HPC chain stiffness.[28] At about 60 wt%, the helix pitch is short enough for the solution to show selective reflection in the red, whereas a blue-shift is observed with increasing concentration[28–31] (Supporting Information, Figure S1). Unfortunately, the viscosity is extremely high at these concentrations, rendering the manipulation of the material particularly challenging.

We envisage that LMs can serve as a miniature and robust platform for the controlled self-assembly of HPC, in aqueous solutions into a cholesteric LC phase that shows selective reflection. To overcome the limitations imposed by high viscosity, we handle the solution at concentrations where the viscosity is manageable. Our strategy consists of first prepar-ing transparent LMs containing an HPC solution at low enough initial polymer concentration c_{init}. This brings the initial HPC solution in the LM into the biphasic regime of the phase diagram, where an isotropic and a cholesteric phase co-exist.[32] By then immersing the LM in a given volume of an organic solvent of minute water miscibility (toluene), a precise amount of water is extracted. As a result, we can quantita-tively tune the final HPC concentration (c_{fin}) in the LM by varying the volume of toluene. Since the equilibrium pitch P of the cholesteric phase is a function of c_{fin}, this means that we

can program P according to desire, resulting in LMs with tailored color. This is a unique demonstration of macroscopic, self-standing soft photonic elements made from a sustainable bio-sourced polymer. We further show that LMs respond with visible color changes, to the application of various external stimuli, such as temperature, mechanical compression, and exposure to toxic chemicals.

Results and Discussion

Preparation of Colored Cholesteric Liquid Marbles

Figure 1 A shows our experimental system. We chose fumed silica NPs with both hydrophilic silanol (33%) and hydrophobic methyl groups on their surface[33] as the LM coating, for two reasons. First, due to their low wettability (air–water contact angle[34] ca. 120˚), they should be suitable LM stabilizers[35] although HPC solutions have considerably lower surface tension (ca. 42 mNm^{-1} for a broad concen-tration range[36]) than pure water. Second, their small size (20–30 nm for individual NPs, few hundred nm for aggregates[37]) ensures a reduction of light scattering and thus optically clear LMs,[38] contrary to other particles typically utilized[39] (Sup-porting Information, Figure S2). We create drops (volume 2 μL) of an aqueous HPC solution at $c_{init} = 55$ wt% (Support-ing Information) that is in the biphasic regime, where an isotropic and a cholesteric phase co-exist (Supporting In-formation, Figure S3), in accordance with earlier work.[32]

We prepare LMs by letting drops roll extensively for 3 min on a bed of the hydrophobic NPs (refractive index $n = 1.46$). We then pick up each LM with a pair of forceps and place them in vials filled with a prescribed volume of toluene ($n = 1.497$), where water extraction then takes place (Supporting Information). If we let the water quickly evaporate under ambient conditions rather than transferring the LM to toluene, this results in non-spherical objects with no structural colors (Supporting Information, Figure S4 and Movie S1). We hypothesize that a slow water extraction and thus a slow concentration increase gives enough time for the polymer molecules to adjust to the concentration change, organizing with a new equilibrium pitch. The immersion in toluene facilitates slow drying of the LM core, on the order of about 9 h for our set of parameters (Figure 1 B; Supporting In-formation, Figure S5 and Movie S2). A similar method was recently used to slowly extract water from cellulose nano-crystal suspensions, resulting in films with homogeneous structural coloration.[40] We chose toluene because it is a non-solvent for HPC, ensuring the integrity of the LM. Further-more, the low solubility of water in toluene (0.045 wt% at 20°C[41]) allows us to control the amount of water that is extracted from the LM, of critical importance for our ability to program the LM color. This is dictated by the volume of the toluene bath (V_{bath}) in which the LM is immersed (Figure 1 B). By varying V_{bath}, we can extract the desired amount of water from the immersed LM and thus reach a desired c_{fin}. Figure 1 C shows LMs with different structural colors. Red, green and blue LMs are typically prepared using V_{bath} of 0.6, 1, and 1.2 mL, respectively (Supporting Information). The LMs
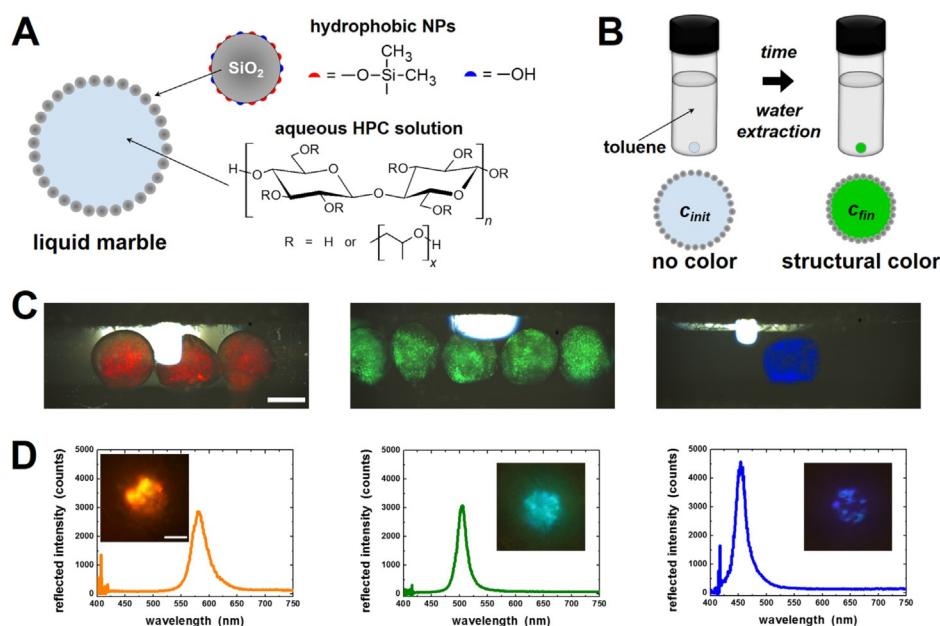
Figure 1. Preparation of liquid marbles (LMs) with tailored structural color. A) Our system: LMs are prepared by rolling drops (initial volume $V_{init} = 2$ μL) of aqueous hydroxypropyl cellulose solutions (initial concentration $c_{init} = 55$ wt.%) on hydrophobized fumed silica nanoparticles. B) Our tailoring concept: LMs are immersed in a toluene bath of volume V_{bath}, the minute solubility of water in toluene allowing a precise amount of water to be slowly extracted from the LM. The final concentration, c_{fin}, and thus the cholesteric pitch, P, is programmed by using the appropriate V_{bath} value. C) Low-magnification reflection micrographs of structurally colored LMs. Collimated white light was shone onto the LMs and images were collected at normal incidence. Red, green and blue LMs are typically prepared by using V_{bath} of 0.6, 1, and 1.2 mL, respectively. The white area is due to specular reflection on the glass vial. Scale bar: 1 mm. D) Reflection spectra (normal incidence) collected from a small area of the LM. The insets are reflection micrographs of these areas. Scale bar: 100 μm.

show multiple light speckles, while having an overall macroscopically uniform color. Other solvents that fulfil the above criteria, such as alkanes (Supporting Information, Figure S6), were also successfully used to obtain LMs with a given color.

So far, apart from colloidal crystallization which also led to selective reflection of white light,[19] colored LMs have only been prepared by either using chromophore-containing[42] or structurally colored[43] encapsulating particles or by adding dyes to the core liquid.[44] Our colored LMs are qualitatively different from these cases. On the one hand, the silica NPs at the LM surface cannot form colloidal crystals because they are very disperse in size and tend to form aggregates instead,[37] hence they do not influence the LM optical properties. This is further supported by our observation that LMs coated with the same NPs, made of pure water or HPC solution with pitch outside the regime of visible structural color (Supporting Information, Figure S2), are colorless. On the other hand, our LMs do not contain any kind of chromophore.[44] To our knowledge, this is the first demonstration of LMs that show structural colors due to a cholesteric liquid crystalline organization of their encapsulated phase.

Optical Response of Cholesteric Liquid Marbles

To quantify the local optical response of our LMs, we recorded reflection spectra (at normal incidence) from a small area (582 μm × 388 μm) of the LM (typical diameter ca. 1.5 mm). Figure 1D shows typical spectra and micrographs (insets) of parts of the sampled areas. The red, green and blue

LMs show maximum reflectance at about 579, 505, and 454 nm, respectively. Based on previous data,[46] we estimated that the average refractive index of the HPC solutions enclosed in our LMs is $n_{av} = 1.42$ for $c_{fin} = 61.1$ wt% (red LM) and $n_{av} = 1.43$ for $c_{fin} = 66.1$ wt% (green LM) and for $c_{fin} = 68.8$ wt% (blue LM; Supporting Information, Table S1). We may assume that the spectra in Figure 1D are predominantly the result of light selectively reflected from regimes with the correct orientation for direct Bragg reflection. This means that the cholesteric helix is oriented along the illumination axis, since we illuminate and analyze along the same direction (we neglect secondary effects such as multiple scattering). We can thus calculate the cholesteric pitch in each LM using Bragg's law and $\alpha = 0°$ (normal incidence). We then find that P equals 408, 354 and 317 nm for the red, green and blue LMs, respectively. These values are significantly larger than the ones published by Werbowyj and Gray[45] (based on their linear fit of $P^{-1/3}$ vs. HPC weight fraction, we should expect P values of 359, 269, 232 nm for our LMs), which may be attributed to the considerably higher degree of substitution (3.6–3.8) of their HPC compared to ours (2.8). Considering reasonable refractive index values, the P values we obtain from spectroscopy match well the colors observed in our LMs, and these colors are in good agreement with reported macroscopic colors observed from the same HPC solutions as the one used here.[31]

Interestingly, the photonic band gap of all LMs is quite narrow, with typical full width at half maximum values ranging from about 33 nm for the red LM to about 24 nm for the blue LM. The reflection bandwidth for a well-aligned

cholesteric is equal to $P\Delta n$,[47] where Δn is the local optical birefringence, that is, $\Delta n = n_{\parallel} - n_{\perp}$, where $n_{\parallel}$ and $n_{\perp}$ are the refractive indices parallel and perpendicular to the director, respectively. HPC has low birefringence, of the order of 0.01,[46] hence for a perfectly aligned sample and perfect normal incidence we would expect an even narrower band gap on the order of 5 nm. The greater band gap observed indicates a certain variation of helix axis within the LM that gives rise to reflection picked up by the spectrophotometer, which samples a non-zero band of incidence angles, broadening the range of reflected colors. Although the spectra shown in Figure 3 were obtained without using polarizers, additional experiments indicated that the LMs selectively reflect circularly polarized light of both right and left handedness. This appears to be in contrast with the right-handed cholesteric mesophase in aqueous HPC solutions.[45] We attribute the fact that we observe both handednesses to the globally random helix orientation in the LM. The perfect right-handedness selection only works for normal incidence, since only then the eigenmodes are truly circular. While regimes where the helix is not in reflection orientation (that is, parallel to the illumination axis) will not give direct reflection, they give rise to birefringence, which can change the handedness of elliptically polarized light of which circular polarization is a special case.[48] The full elucidation of the optical behavior of our LMs is beyond the scope of this paper and will be the subject of future work.

Macroscopically, the LMs display iridescence: by increasing the angle between the illumination and viewing directions, we observe a gradual color variation to shorter wavelengths. To characterize the angle-dependent selective reflection, we use a fixed horizontal microscope and a movable light source illuminating the LMs that were contained in vials with toluene (Figure 2A). We define φ as the angle between the microscope and the illumination axis. Figure 2B shows that the LM color is blue-shifted with increasing φ; the LM, orange at normal incidence ($\varphi = 0°$), becomes yellowish at $\varphi = 45°$ and green at $\varphi = 75°$. Interestingly, a dark green color is observed for $\varphi = 90°$, indicating that the color must be the result of light being reflected from the LM interior. The same behavior was observed in a green LM as φ was varied (Supporting Information, Figure S7), indicating that the angle-dependent selective reflection is a generic property of the cholesteric LMs.

Microstructure of Cholesteric Liquid Marbles

Optical micrographs reveal the structural and morphological characteristics of LMs (Figure 2C). The transmission image (top, left) shows the high transparency of the LM. Polarized optical microscopy (top, right, and bottom) reveals a grainy structure comprising small regimes (ca. 5–10 μm large) of uniform color. This indicates that the cholesteric helix follows random directions in the LM interior. The more uniform color at distances of about 25 μm from the LM surface (bottom) suggests that the helix has a more uniform alignment near the LM edge. This is presumably due to an alignment effect from the coating NPs and the surrounding toluene, which are both highly hydrophobic.

Based on the above observations, we propose the LM structure shown in Figure 2D. Our main assumption is that P
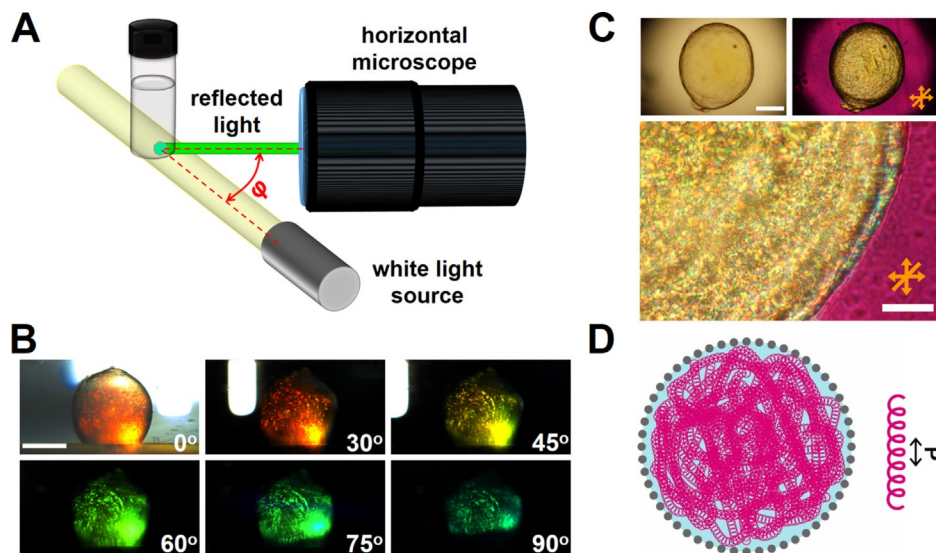

Figure 2. The optical properties of the structurally colored LMs result from their cholesteric helical structure. A) The setup used to measure the angular dependence of the selective reflection of white light from LMs; φ is the angle between the illumination and detection axes. B) Reflection micrographs show that the reflected wavelength undergoes a blue shift with increasing φ from 0° (normal incidence) to 90°. Scale bar: 500 μm. C) Typical transmission images of a structurally colored LM. The brightfield image (top left panel) shows that the LM is spherical and transparent. Imaging between crossed polarizers and a wave plate (top right and bottom panels) reveals regimes with different orientations of the cholesteric helix across the LM. Scale bars: 500 μm (top images) and 100 μm (bottom image). D) Our proposed scenario for the internal structure of the LMs. The polymer molecules self-assemble into a cholesteric structure with a constant helical pitch P, but the orientation of the helix varies randomly throughout the LM. Drawing a qualitative analogy to the powder X-ray diffraction of a polycrystalline solid, in which the lattice orientation varies randomly throughout the sample, this results in a powder-like character of our LM. For simplicity, we draw only helix orientations within the paper plane, while in reality they probe all 3D space.

is constant throughout the LM, and it is solely defined by c_{fin} at a given T.[32] The continuous cholesteric helix, which spans the whole LM volume, adopts all possible orientations. Regimes with different helix orientation yield different optical properties, producing the grainy LM appearance in the polarized optical microscopy images (Figure 2C). As a result, the average refractive index, n_{av}, is the same everywhere in the LM. When collimated white light impinges on the LM, and for a given angle φ between the illumination and viewing axes, selective reflection occurs. Given that P and n_{av} are fixed, all helix orientations for which $\alpha < 90°$ will lead to selective reflection by Bragg's law. Since we have a slight spread of illumination directions and we integrate over a spread of viewing directions, we get a certain reflection bandwidth (Figure 1D). For simplicity reasons, our model of the LM does not consider the possible alignment of the cholesteric helix near the LM surface, because this effect extends to distances of about 25 μm, negligible compared to the LM diameter (mm scale). We also omit in our schematic the presence of defects in the cholesteric structure, which we nevertheless expect to have in large numbers.[49] We have recently proposed a similar internal structure for rubber fibers (with much smaller diameters, of about 100 μm) containing a thermotropic liquid crystal core, to explain their optical response that is similar to the one reported here for LMs.[50]

It is remarkable that the lyotropic HPC/water system does not require a uniform helix alignment to show uniform structural color. This is in stark contrast to thermotropic LC samples of comparable size which require a uniform alignment of the cholesteric helix to show strong and uniform color, as seen in drops or shells.[51] In the latter case, the anchoring at the external and internal surfaces dictates a well-defined director profile. Realizing shells of macroscopic dimensions can be challenging, however. Hence if one wishes to fabricate a large spherical photonic reflector, a drop is easier to make but one must then deal with the (unavoidable) overall disordered structure comprising LC domains with random orientations and the consequent problem of light scattering. The scattered light arises from adjacent domains with different helix orientations which, due to birefringence, have large refractive index mismatch in case of thermotropics (birefringence an order of magnitude larger than HPC solutions). We thus expect that any macroscopic object that is made of randomly aligned cholesteric domains of a thermotropic LC will always have a white appearance. We confirmed this by preparing LMs with a thermotropic mixture (ROTN-615 with 25 wt% chiral dopant R811) that forms short-pitch cholesteric mesophases: these LMs had an appearance similar to mother of pearl, where strong light scattering and only weak structural colors could be seen. On the contrary, the scattering intensity is low in the case of our LMs, because of the low birefringence of HPC solutions.

Color Response to Temperature

A noteworthy property of cholesteric aqueous HPC solutions is the dependence of their optical properties on temperature T. The structural color is shifted to longer wavelengths upon heating,[28,32] however the underlying physical mechanism remains unclear. We therefore expect that our colored LMs should have a T-dependent optical response. To test this, we recorded the reflection spectra at normal incidence of an LM (immersed in toluene) at different T (Figure 3A). At 25°C, the LM is green with a peak in reflection intensity at $\lambda_{max} = 499$ nm. Upon cooling, λ_{max} progressively shifts to lower values, going from 466 nm at 20°C to 442 nm at 15°C, reaching 424 nm at 10°C. Although our spectrometer cannot measure shorter wavelengths, we observe that further cooling turns the LM colorless; we attribute this to λ_{max} entering the UV range. Conversely, a gradual red shift of λ_{max} is observed upon heating. For the highest T measured (45°C), $\lambda_{max} = 615$ nm. We did not explore higher T because of the proximity to the lower critical solution temperature, above which macroscopic phase separation into a polymer-rich and a solvent-rich phase occurs.[32] In fact, it may be that the broad secondary peak appearing at longer wavelengths at high T is related to phase separation.

We observe a linear increase of λ_{max} with T with a slope $d\lambda_{max}/dT = 5.7$ nm/°C, highlighting the high sensitivity of P and thus of the photonic band gap to T (Figure 3B). We can
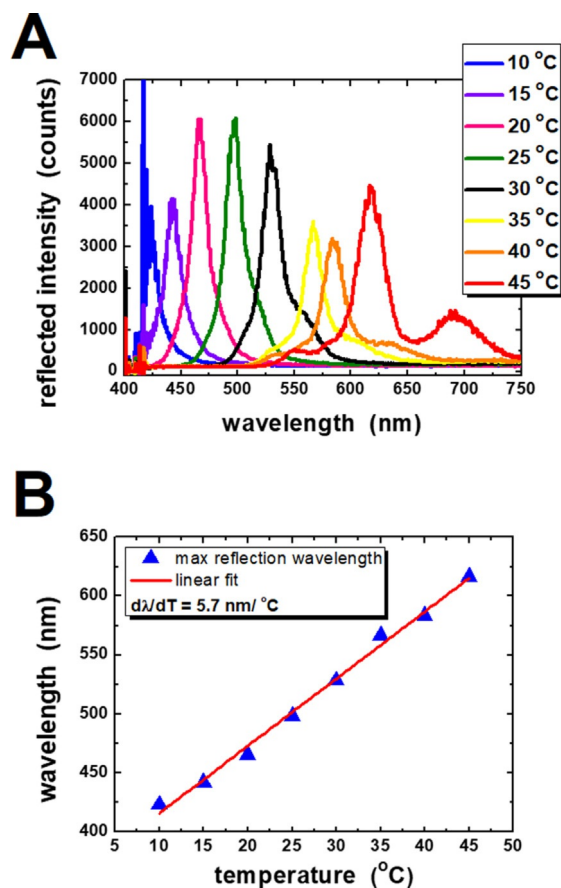
Figure 3. Real-time tuning of the LM structural color with temperature (T). A) Reflection spectra (at normal incidence) of the same LM at different T. This green LM ($V_{init} = 2$ μL, $c_{init} = 55$ wt%) was prepared by using a toluene bath of $V_{bath} = 1$ mL. The experiments were performed with the LM immersed in the toluene bath. The reflection peak is red (resp. blue) shifted with increasing (resp. decreasing) T. B) Maximum reflected wavelength as a function of T. The red line is a linear fit to the data.

exclude that the thermal sensitivity of the LM color results from the T-dependent solubility of water in toluene: the latter increases with increasing T,[41] hence the HPC concentration in the LM would increase with increasing T, which would in turn lead to a blue shift (Figure 1 and Supporting Information). We observe the opposite, that is a red shift of the selective reflection upon LM heating. We instead believe that the T sensitivity of hydrogen bonding (both intermolecular between adjacent chains and between chains and water molecules) may be responsible for this effect. The linear dependence of λ_{max} with T is in qualitative agreement with earlier reports, which also attributed it to the increase of P with T.[27,28] Our $d\lambda_{max}/dT$ is higher than the value reported earlier[28] which was about 1.5 nm/°C, and this may be due to the reported complex dependence of $\lambda_{max}(T)$ on HPC concentration and the specific characteristics of the HPC used in different studies[29] or to the slow dynamics of concentrated HPC solutions, making it difficult to judge when equilibrium has been reached after changing T. Interestingly, the T-driven color tuning of our LMs is achieved in real-time: typically, LMs change color only a few seconds after a T change, most likely related to their small volume.

Patterning of Liquid Marbles in a Polymer Matrix

LMs that have reached the designated c_{fin} inside a given V_{bath} are highly sensitive to any type of external perturbation. For example, although LMs maintain their color when kept in tightly sealed vials, even brief opening of the vial with minute

evaporation of toluene vapor leads to a blue shift. We attribute this color change to more water having escaped the LM than programmed; leakage of water-saturated toluene vapor from the vial causes more water to leave the LM. We have devised a simple strategy to pattern LMs within a solid polymer matrix to preserve their color (Figure 4 A; Supporting Information, Figure S8). We prepare solid polydimethylsiloxane wells on a silicon wafer and we pour optical adhesive into them. We position 17 LMs in the liquid adhesive to form the pattern LUX. Figure 4 A, top panel, shows the resulting pattern after UV curing the optical adhesive ($n = 1.56$). Although we choose red, green, and blue LMs to form the letters L, U, and X, respectively, the patterned LMs show color variations. For example, the letter L is comprised of both orange and yellow LMs. Both water evaporation and mechanical deformation during either LM handling or LM compression as the matrix is cured leads some of them to blue-shift. This is a manifestation of the high sensitivity of these LMs, which respond to various perturbations by easily detectable color changes. Remarkably, the thermoresponsive character of the LMs is maintained even after they are embedded in the solid matrix. Figure 4 A, bottom panel, shows that the color of all LMs is red shifted upon heating (Supporting Information, Movie S3). The LMs of the letter L, orange/red at 25°C, become almost invisible at 45°C, suggesting a shift of λ_{max} to the infrared. At the same time, the LMs of the letter X, violet at 25°C, turn red and yellowish at 45°C. Conversely, cooling the LUX pattern results in a blue-shift of λ_{max} (Supporting Information, Figure S8 and Movie S4). Interestingly, some LMs do not have a single color
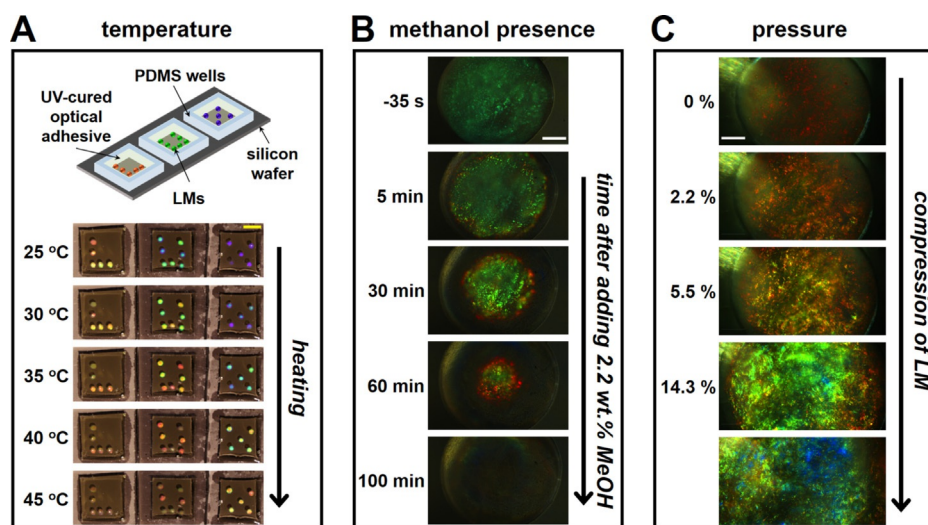

Figure 4. LMs respond to various external perturbations by changing their structural color. A) Top: LMs are placed in wells containing a liquid optical adhesive to form the pattern LUX. UV curing results in a solid matrix containing the LM array. Bottom: Photographs of the LM pattern upon heating, captured with the camera being placed perpendicular to the pattern and white light shone at an angle of about 70°. Scale bar: 5 mm. B) Reflection micrographs showing the color change of a green LM ($V_{init} = 8\ \mu L$, $c_{init} = 55\ wt\%$) after a drop of methanol (100 μL) is added to the toluene bath ($V_{bath} = 4\ mL$, methanol concentration 2.2 wt%) in which the LM was prepared. At $t = 0$, methanol is added to the toluene bath. Scale bar = 500 μm. C) Reflection micrographs of a red LM ($V_{init} = 10\ \mu L$, $c_{init} = 55\ wt\%$, $V_{bath} = 4\ mL$) that is uniformly compressed using the setup shown in the Supporting Information, Figure S10. $t = 0$ corresponds to the instant when the LM starts to be compressed. Snapshots corresponding to increasing levels of compression are shown. The values of the relative changes of the LM horizontal radius, defined as $\frac{R_{exp} - R_{init}}{R_{init}}$, where R_{init} and R_{exp} are, respectively, the initial LM radius and the expanded radius in the horizontal direction (that is, in the sample plane) upon compression. Note that the value for maximum compression (bottom panel) cannot be calculated, because the expanded LM diameter is larger than the field of view. Scale bar: 500 μm. The images in (B), (C) were acquired with the objective perpendicular to the LMs and white light shone at an angle of about 45° with respect to the imaging axis.

at a given *T*; instead, a broad central spot of one color is surrounded by a ring of a color corresponding to shorter wavelengths. This suggests that there might still be kinetic evolution of the polymer ordering, which we will explore in the future. Interestingly, we observe a similar behavior when the array is heated by skin temperature or cooled down by evaporative cooling (Supporting Information, Figure S9 and Movie S5). These observations suggest that the reversible *T*-induced color changes cannot be due to water diffusing from/to the LM. Overall, our findings demonstrate that cholesteric LMs can be easily manipulated to yield macroscopic, stimuli-responsive devices.

Color Response to Exposure to Methanol

Based on the above observations, we anticipated that LMs might be able to sense the presence of chemicals in their environment. To test this, we add a small amount of methanol (concentration 2.2 wt% in the bath) in the vial where a large green LM has been prepared (Figure 4B). Within $t = 1$ min after methanol addition, the LM responds by a decrease in the intensity of the selectively reflected light that initially remains green overall (Supporting Information, Figure S11 and Movie S6). At longer times, a circular region of bright green color appears (5 min), which propagates to the LM center. Later on, red spots appear at the periphery of this region (10–30 min), which shrinks with time until an almost completely red circle is observed (60 min). The overall red shift is presumably due to the decrease of HPC concentration in the LM caused by the diffusion of methanol, which is both water-miscible and a good solvent for HPC.[32] As a result of this dilution, the equilibrium pitch increases. We expect that the presence of any solvent in the LM environment that is both miscible with water and a good solvent for HPC (such as ethanol, acetone, tetrahydrofuran) would produce similar color changes. We further attribute the radial evolution of color change to the kinetics of methanol diffusion from the toluene bath to the LM interior. It follows that the characteristic timescale of the color change of the LM upon exposure to methanol, much slower than the case of thermal and mechanical stimulation (several min vs. s), is dictated by the kinetics of methanol diffusion. These results highlight the potential of using LMs as miniature sensors for detecting the presence of toxic chemicals.

Color Change upon Mechanical Compression

Bearing in mind that the optical properties of cholesteric HPC solutions are sensitive to pressure,[52] we investigate the response of cholesteric LMs under compression (Figure 4C; Supporting Information, Figures S10, S12). A large LM, which is red in its unperturbed state (relative LM horizontal radius change of 0%), turns consequently orange, yellow–orange, green, and green–blue with increasing compression (relative LM horizontal radius change from 2.2% to above 14.3%). The pressure-induced color change is almost instantaneous, with a corresponding time scale of about 1 s. It is also reversible, as evidenced from the LM returning to its unperturbed state, recovering both its initial shape and color. However, the kinetics of the color and shape recovery processes generally differ: for weak deformations, both the color and the shape are quickly recovered, whereas for strong deformations the color is recovered much faster than the shape (Supporting Information, Figure S12 and Movie S7). This hysteresis suggests that the color change is transient and not the result of a new equilibrium state of the cholesteric structure upon compression. We speculate that compression affects both the cholesteric pitch and the orientation of the cholesteric domains, as has been previously suggested.[31,52] In thick, flat films of aqueous HPC solutions, the application of pressure leads to a macroscopic blue shift of the selective reflection, which is the result of the shortened average pitch. However, additional effects occur at the microscale. Vertical compression of locally tilted domains (with respect to the film surface) may lead to either an increase or decrease of the pitch (corresponding to red and blue shift, respectively), depending on the helix orientation relative to the vertical compression. Furthermore, the generated lateral shear flow can also misalign the cholesteric domains, which gives rise to the broadening of the reflection spectrum.[31] The fact that our LMs have a spherical geometry implies that the stress distribution should be different than in the case of flat films. Further research is needed for a complete elucidation of the LM optical response to pressure, but we expect that the above phenomena might play an important role. To sum up, the mechanochromic response of our LMs indicates their potential to be exploited in cost-effective pressure-sensing applications.[31]

Conclusion

We report here for the first time the self-assembly of a bio-derived polymer in water into a cholesteric liquid crystalline phase inside liquid marbles (LMs). From a fundamental viewpoint, LMs emerge as a unique, miniature and precisely controlled experimental platform for realizing and studying solvent-dependent liquid crystalline self-assembly of a highly viscoelastic system, in much shorter times than in conventional experiments (hours versus weeks). From a practical perspective, this new concept provides a simple yet robust method for preparing soft spheres with tailored structural colors, at a length-scale (millimeters) that has never been achieved before. This is due to the inherent low birefringence of HPC solutions, which removes the necessity of a well-aligned helix orientation. The narrow photonic band gap of these reflectors can be pre-programmed by precisely engineering the drying process. Furthermore, these independent, self-standing photonic soft objects respond to various external stimuli by visual color changes: 1) LMs show a real-time red (resp. blue) color shift upon heating (resp. cooling) that spans the complete visible spectrum, entering the IR (UV) range as well; 2) LMs sense the presence of methanol in their environment by showing a blue shift of the reflected wavelength; 3) LMs sense the pressure applied on them by blue shifting their color in real-time. Our LMs resemble the performance

of thermotropic liquid crystals under confinement, however without the issues of high cost and toxicity that typically accompany synthetic thermotropic systems. This may open the route of using LMs made of sustainable bio-derived materials in a new generation of cost-effective, environmentally friendly, and sustainable sensors and soft photonic elements.

[1] P. Aussillous, D. Quéré, *Nature* **2001**, *411*, 924 – 927.
[2] S. U. Pickering, *J. Chem. Soc. Trans.* **1907**, *91*, 2001 – 2021.
[3] B. P. Binks, R. Murakami, *Nat. Mater.* **2006**, *5*, 865 – 869.
[4] B. P. Binks, *Curr. Opin. Colloid Interface Sci.* **2002**, *7*, 21 – 41.
[5] G. McHale, M. I. Newton, *Soft Matter* **2011**, *7*, 5473 – 5481.
[6] E. Bormashenko, *Langmuir* **2017**, *33*, 663 – 669.
[7] P. Aussillous, D. Quéré, *Proc. R. Soc. London Ser. A* **2006**, *462*, 973 – 999.
[8] C. H. Ooi, N. T. Nguyen, *Microfluid. Nanofluid.* **2015**, *19*, 483 – 495.
[9] S. Fujii, S. Yusa, Y. Nakamura, *Adv. Funct. Mater.* **2016**, *26*, 7206 – 7223.
[10] Y. Zhao, J. Fang, H. Wang, X. Wang, T. Lin, *Adv. Mater.* **2010**, *22*, 707 – 710.
[11] J. Vialetto, M. Hayakawa, N. Kavokine, M. Takinoue, S. N. Varanakkottu, S. Rudiuk, M. Anyfantakis, M. Morel, D. Baigl, *Angew. Chem. Int. Ed.* **2017**, *56*, 16565 – 16570; *Angew. Chem.* **2017**, *129*, 16792 – 16797.
[12] N. Kavokine, M. Anyfantakis, M. Morel, S. Rudiuk, T. Bickel, D. Baigl, *Angew. Chem. Int. Ed.* **2016**, *55*, 11183 – 11187; *Angew. Chem.* **2016**, *128*, 11349 – 11353.
[13] M. Paven, H. Mayama, T. Sekido, H. J. Butt, Y. Nakamura, S. Fujii, *Adv. Funct. Mater.* **2016**, *26*, 3199 – 3206.
[14] E. Bormashenko, Y. Bormashenko, A. Musin, Z. Barkay, *ChemPhysChem* **2009**, *10*, 654 – 656.
[15] J. Tian, T. Arbatan, X. Li, W. Shen, *Chem. Commun.* **2010**, *46*, 4734 – 4736.
[16] H. K. Lee, Y. H. Lee, I. Y. Phang, J. Wei, Y. E. Miao, T. Liu, X. Y. Ling, *Angew. Chem. Int. Ed.* **2014**, *53*, 5054 – 5058; *Angew. Chem.* **2014**, *126*, 5154 – 5158.
[17] Y. Xue, H. Wang, Y. Zhao, L. Dai, L. Feng, X. Wang, T. Lin, *Adv. Mater.* **2010**, *22*, 4814 – 4818.
[18] G. McHale, M. I. Newton, *Soft Matter* **2015**, *11*, 2530 – 2546.
[19] H. Gu, B. Ye, H. Ding, C. Liu, Y. Zhao, Z. Gu, *J. Mater. Chem. C* **2015**, *3*, 6607 – 6612.
[20] J. D. Forster, H. Noh, S. F. Liew, V. Saranathan, C. F. Schreck, L. Yang, J. C. Park, R. O. Prum, S. G. J. Mochrie, C. S. O'Hern, H. Cao, E. R. Dufresne, *Adv. Mater.* **2010**, *22*, 2939.
[21] Y. Zhao, L. Shang, Y. Cheng, Z. Gu, *Acc. Chem. Res.* **2014**, *47*, 3632 – 3642.
[22] C. W. Oseen, *Trans. Faraday Soc.* **1933**, *29*, 883.
[23] H. de Vries, *Acta Crystallogr.* **1951**, *4*, 219 – 226.
[24] A. P. C. Almeida, J. P. Canejo, S. N. Fernandes, C. Echeverria, P. L. Almeida, M. H. Godinho, *Adv. Mater.* **2018**, *30*, 1703655.
[25] M. Mitov, *Soft Matter* **2017**, *13*, 4176 – 4209.
[26] E. D. Klug, *Encycl. Polym. Sci. Technol.* **1971**, 307 – 314.
[27] R. S. Werbowyj, D. G. Gray, *Mol. Cryst. Liq. Cryst.* **1976**, *34*, 97 – 103.
[28] R. S. Werbowyj, D. G. Gray, *Macromolecules* **1980**, *13*, 69 – 73.
[29] S. Fortin, G. Charlet, *Macromolecules* **1989**, *22*, 2286 – 2292.
[30] M. H. Godinho, P. Pieranski, P. Sotta, *Eur. Phys. J. E* **2016**, *39*, 89.
[31] H. L. Liang, M. M. Bay, R. Vadrucci, C. H. Barty-King, J. Peng, J. J. Baumberg, M. F. L. De Volder, S. Vignolini, *Nat. Commun.* **2018**, *9*, 4632.
[32] S. Guido, *Macromolecules* **1995**, *28*, 4530 – 4539.
[33] B. P. Binks, S. O. Lumsdon, *Langmuir* **2000**, *16*, 8622 – 8631.
[34] T. Kostakis, R. Ettelaie, B. S. Murray, *Langmuir* **2006**, *22*, 1273 – 1280.
[35] D. Zang, Z. Chen, Y. Zhang, K. Lin, X. Geng, B. P. Binks, *Soft Matter* **2013**, *9*, 5067 – 5073.
[36] S. A. Chang, D. G. Gray, *J. Colloid Interface Sci.* **1978**, *67*, 255 – 265.
[37] M. Anyfantakis, D. Baigl, B. P. Binks, *Langmuir* **2017**, *33*, 5025 – 5036.
[38] P. S. Bhosale, M. V. Panchagnula, H. A. Stretz, *Appl. Phys. Lett.* **2008**, *93*, 034109.
[39] P. Singha, S. Swaminathan, A. S. Yadav, S. N. Varanakkottu, *Langmuir* **2019**, *35*, 4566 – 4576.
[40] T. H. Zhao, R. M. Parker, C. A. Williams, K. T. P. Lim, B. Frka-Petesic, S. Vignolini, *Adv. Funct. Mater.* **2018**, 1804531.
[41] C. K. Rosenbaum, J. H. Walton, *J. Am. Chem. Soc.* **1930**, *52*, 3568 – 3573.
[42] A. M. Fernandes, D. Mantione, R. Gracia, J. R. Leiza, M. Paulis, D. Mecerreyes, *ACS Appl. Mater. Interfaces* **2015**, *7*, 4433 – 4441.
[43] Y. Zhao, H. Gu, Z. Xie, H. C. Shum, B. Wang, Z. Gu, *J. Am. Chem. Soc.* **2013**, *135*, 54 – 57.
[44] F. Geyer, Y. Asaumi, D. Vollmer, H. J. Butt, Y. Nakamura, S. Fujii, *Adv. Funct. Mater.* **2019**, *29*, 1808826.
[45] R. S. Werbowyj, D. G. Gray, *Macromolecules* **1984**, *17*, 1512 – 1520.
[46] Y. Onogi, Y. Nishijima, *Kobunshi Ronbunshu* **1986**, *43*, 223.
[47] J. L. Fergason, *Mol. Cryst.* **1966**, *1*, 293 – 307.
[48] H. Takezoe, Y. Ouchi, M. Hara, A. Fukuda, E. Kuze, *Jpn. J. Appl. Phys. Part 1* **1983**, *22*, 1080 – 1091.
[49] D. Seč, S. Čopar, S. Žumer, *Nat. Commun.* **2014**, *5*, 3057.
[50] L. W. Honaker, S. Vats, M. Anyfantakis, J. P. F. Lagerwall, *J. Mater. Chem. C* **2019**, *7*, 11588 – 11596.
[51] M. Urbanski, C. G. Reyes, J. Noh, A. Sharma, Y. Geng, V. Subba Rao Jampani, J. P. F. Lagerwall, *J. Phys. Condens. Matter* **2017**, *29*, 133003.
[52] G. Kamita, B. Frka-Petesic, A. Allard, M. Dargaud, K. King, A. G. Dumanli, S. Vignolini, *Adv. Opt. Mater.* **2016**, *4*, 1950 – 1954.